Agricultural and Forest Meteorology 189–190 (2014) 81–90

Contents lists available at ScienceDirect

Agricultural and Forest Meteorology

journal homepage: www.elsevier.com/locate/agrformet

Spatial and temporal variations in the end date of the vegetation growing season throughout the Qinghai–Tibetan Plateau from 1982 to 2011

Mingliang Che[a,b], Baozhang Chen[a,c,*], John L. Innes[c], Guangyu Wang[c], Xianming Dou[d], Tianmo Zhou[e], Huifang Zhang[a,b], Jianwu Yan[a,b], Guang Xu[a,b], Hongwei Zhao[a,b]

[a] State Key Laboratory of Resources and Environmental Information System, Institute of Geographical Sciences and Natural Resources Research (IGSNRR), Chinese Academy of Sciences (CAS), Beijing 100101, China
[b] University of Chinese Academy of Sciences, Beijing 100049, China
[c] Department of Forest Resource Management, University of British Columbia, 2424 Main Mall, Vancouver, BC, Canada V6T 1Z4
[d] School of Resources and Earth Sciences, China University of Mining and Technology, Xuzhou 221116, China
[e] Key Lab of Resources Environment and GIS, Capital Normal University, Beijing 100048, China

ARTICLE INFO

Article history:
Received 7 September 2013
Received in revised form
30 December 2013
Accepted 3 January 2014

Keywords:
Autumn phenology
End date of the vegetation growing season (EGS)
Spatial–temporal variation
AVHRR LAI
Qinghai–Tibetan Plateau

ABSTRACT

The spatial and temporal variations in the end date of the vegetation growing season (EGS) and their relationships with climate factors across the Qinghai–Tibetan Plateau yet have not been well researched. In this study, we used the rate of the change in the curvature of the *S*-curve function which integrated a logistic function and an asymmetric Gaussian function and showed a better performance for fitting the LAI (leaf area index) data to extract the EGS from a long-term time series of AVHRR (advanced very high resolution radiometer) LAI data. The spatial distribution pattern of the EGS averaged from 1982 to 2011 presented a gradual decrease from the southeast to northwest plateau. The various vegetation types showed different phenological EGS timing. The EGS occurred earlier with increasing altitude (slope = −3 day km^{-1}, $p < 0.001$). Throughout the entire Qinghai–Tibetan Plateau, the monthly air temperature and precipitation were positively correlated with the EGS, whereas the monthly sunshine duration showed a negative correlation. At the regional scale, a less pronounced increasing EGS trend (shifting about 1 day over 24 years, $p = 0.084$) was observed during the entire study period. By analyzing the trend turning points, we found that the EGS occurred later during 1982–1994 (slope = 0.155 day yr^{-1}, $p = 0.045$) and 1999–2011 (slope = 0.096 day yr^{-1}, $p = 0.3$), but occurred earlier during 1994–1999 (slope = −0.373 day yr^{-1}, $p = 0.049$). During 1982–2011, the annual changes of EGS negatively correlated with precipitation ($p < 0.1$) in June, but positively with precipitation ($p < 0.1$) in August. As the same time, the annual changes of EGS positively correlated with sunshine duration ($p < 0.1$) in June, yet negatively with sunshine duration ($p < 0.1$) in August. During 1982–1994, the annual changes of EGS positively correlated with air temperature ($p < 0.01$) and negatively with precipitation ($p < 0.1$) in June. During 1994–1999, the annual changes of EGS only negatively correlated with air temperature ($p < 0.05$) in August. During 1999–2011, the annual changes of EGS only negatively correlated with sunshine duration ($p < 0.1$) in August.

1. Introduction

Vegetation phenology is defined as the seasonal timing of life cycle events in plants as influenced by weather and climate, especially temperature (Richardson et al., 2006; Schwartz, 2003; White et al., 1997). Vegetation phenology is critical for plant survival and production under shifting environmental conditions (Rathcke and Elizabeth, 1985) and thus is a robust indicator of the effects of climate change (Richardson et al., 2006; White et al., 1997). During the vegetation phenophases, the end date of the growing season (EGS), i.e. the end of the vegetation senescence (or defoliation) or the start of the vegetation dormancy, is a very important index that determines the length of the growing season (LGS) and also controls the spatial–temporal dynamics of critical carbon and water cycles (Jong et al., 2011; White et al., 1997).

Numerous studies have revealed that the EGS has occurred later in the recent half century. For example, Menzel and Fabian (1999) reported that autumn phenology events were delayed by 4.8 days

* Corresponding author at: Institute of Geographical Sciences and Natural, Resources Research, Chinese Academy of Sciences, Beijing 100101, China. Tel.: +86 01 64889574.
E-mail address: baozhang.chen@igsnrr.ac.cn (B. Chen).

0168-1923/$ – see front matter © 2014 Elsevier B.V. All rights reserved.
http://dx.doi.org/10.1016/j.agrformet.2014.01.004

from 1959 to 1993 in Europe. Zeng et al. (2011) demonstrated the EGS was delayed by 2.2 days in northern America in the last 10 years. Piao et al. (2006) indicated that dormancy was delayed in autumn by 0.37 days yr^{-1} from 1982 to 1999 in China's temperate region. Jeong et al. (2011) reported that at a hemispheric scale the EGS was delayed by 4.3 days during 1982–1999 and further delayed by an additional 2.3 days in the period of 2000–2008. In addition, many studies have analyzed the relationship of EGS with temperature and precipitation and indicated the temperature in autumn typically showed positive correlations with the EGS (Jeong et al., 2011; Zeng et al., 2011). In addition, in tropical ecosystems, autumn phenology might be more closely linked to seasonal shifts in precipitation (Cleland et al., 2007; Reich, 1995). In arid or semi-arid areas, precipitation is also more important than temperature for vegetation growth.

The results of certain studies are not always in agreement with the aforementioned trends of EGS changes. For example, Pudas et al. (2008) indicated there was neither an advancing nor a delaying trend of EGS in Finland during 1997–2006. And Menzel et al. (2001) reported trends of EGS of trees at neighboring stations in Germany often showed contradictory signals. These heterogeneous patterns of EGS changes might be attributed to the differences in study areas. Because of the complexity of terrestrial ecosystems, different study areas have diverse climate features. Moreover, the timing of phenology events is sensitive to climate change (Richardson et al., 2006). Thus, it is clear that EGS variation is strongly dependent on study area.

The Qinghai–Tibetan Plateau is the highest and largest plateau on Earth, and the vegetation in this area is highly sensitive to climate change (Dong et al., 2012; Piao et al., 2011; Shen et al., 2011; Zhang et al., 2013). The unique climate features here, e.g., the intense solar radiation, the longer sunshine duration, the lower air temperature and pressure, the less cloud cover, the obvious seasonal and spatial inhomogeneity of rainfall, etc., make the plateau become the main local driver and amplifier of global climate change (Liu and Chen, 2000; Dong et al., 2012). To date, several studies on the EGS in the Qinghai–Tibetan Plateau have been published (Ding et al., 2012; Dong et al., 2012; Jin et al., 2013; Yu et al., 2010). These studies mainly focused on the spatial distribution and inter-annual changes in the EGS. Some of them analyzed the relationships between the EGS and temperature (Jin et al., 2013; Yu et al., 2010) and altitude (Ding et al., 2012; Dong et al., 2012). However the results of these studies were not always in agreement, such as the opposite inter-annual trends of the EGS between the findings of Dong et al. (2012) and Yu et al. (2010) during 1982–2006, and the inconsistent relationship of the EGS with altitude between the results of Ding et al. (2012) and Dong et al. (2012). Moreover none of these studies analyzed the relationship between the EGS and precipitation and sunshine duration. In fact, many studies have indicated that the precipitation and sunshine duration in the plateau played important roles in the vegetation growth (Kang et al., 2010; Mao et al., 2007; Zhou et al., 2007). Thus, researching the spatial and temporal variations in the EGS and exploring their relationships with climate factors throughout the Qinghai–Tibetan Plateau have been really scarce up to now. This inadequacy has severely restricted our comprehension of the autumn phenology and the whole growing season of the Qinghai–Tibetan Plateau.

In this study, we sought to quantify the spatial and temporal variations of the EGS in autumn at the Qinghai–Tibetan Plateau from 1982 to 2011. More specifically, this study attempted to address the following questions:

(1) What was the spatial distribution of the EGS from 1982 to 2011 on the Qinghai–Tibetan Plateau?
(2) How do the spatial patterns of the EGS correlate with terrain and climate factors?
(3) What were the temporal changes in the EGS over the last 30 years?
(4) What were the spatial patterns of temporal changes in the EGS over the whole plateau?
(5) How do temporal changes in the EGS correlate with climate factors?

2. Data and methods

2.1. Study area

The Qinghai–Tibetan Plateau is located in southwest China (25–40° N and 76–104° E). As the Third Pole of the World, with a mean elevation of higher than 4000 m above sea level and a terrain inclining from northwest to southeast, it has a typical alpine climate and vegetation types (Fig. 1). The mean air temperature throughout the entire plateau is approximately −6.4 °C in winter (from November to January) and −3.4 °C in early spring (February and March) but reaches 10.5 °C in summer (from May to July) and 8.2 °C in autumn (from August to October). The spatial distribution of precipitation over the area is highly variable. Like most regions in China, the precipitation decreases from southeast to northwest. The temporal distribution of precipitation is also uneven, and the rainy season (from May to September) accounts for 60–70% of the annual precipitation (Ye et al., 2013). The vegetation types consist mainly of grass, forest and shrub (Shen et al., 2011) (Fig. 1). In addition, the grass, including meadows and steppe, is dominant and occupies approximately 63.6% of the plateau, mostly distributing in the central part (Piao et al., 2011). Most vegetation occupying 67.7% over the plateau are seasonally deciduous, and less vegetation are evergreen which only account for approximately 4.75% of the plateau (Ran et al., 2009). The growth cycle of the seasonally deciduous vegetation in most area is single, and the growing season ranges from April to October, and the corresponding growth peak occurs during July and August (Ma et al., 2011).

2.2. Datasets

Leaf area index (LAI) can effectively reflect seasonal variations in vegetation. In this study, the LAI dataset at a spatial resolution of 1/12 degree (nearly 0.08 degree) and a 15-day interval, spanning the period from 1982 to 2011, was used. This dataset was generated from AVHRR (advanced very high resolution radiometer), GIMMS (global inventory modeling and mapping studies) NDVI-3g (normalized difference vegetation index, third generation) data (Zhu et al., 2013). To scale the LAI temporal frequency down from 15 days to 1 day, we used the cubic spline interpolation which had a better smooth feature and effectively reflected the signals of original LAI data (Borak and Jasinski, 2009; Xu et al., 2012) to interpolate the missing data. At the same time, for the purpose of minimizing noisy LAI data, which can be caused by deserts, sparsely vegetated areas or other factors, we regarded pixels with LAI value less than 0.2 as invalid. In addition, the observed gross primary productivity (GPP) by the Haibei eddy flux tower was applied to validate the retrieved phenological results. The Haibei station lies in a large valley surrounded by the Qilian Mountain at latitude 37.08° N and longitude 101.08° E. These GPP data were obtained by digitizing GPP plots reported in the literature (Li et al., 2007).

Monthly meteorological data from 57 meteorological stations distributed throughout the plateau (Fig. 1) were obtained from the China Meteorological Data Sharing Service System (http://cdc.cma.gov.c). These data, which span the period of

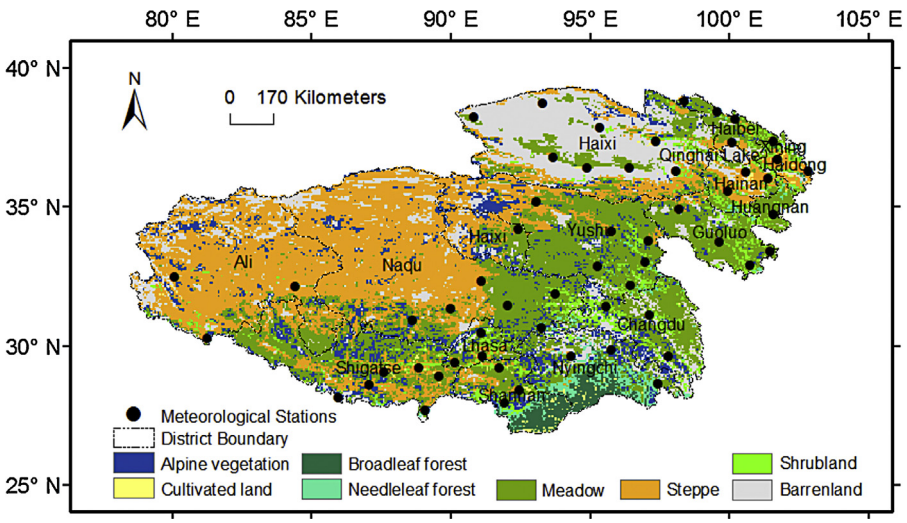

Fig. 1. Spatial distribution of meteorological stations and vegetation types on the Qinghai–Tibetan Plateau.

1982–2011, included the monthly mean surface air temperature, monthly total precipitation and monthly sunshine duration.

Terrain information for the Qinghai–Tibetan Plateau was obtained from the NASA shuttle radar topographic mission (SRTM)-produced digital elevation data (DEM) with 90-m resolution (http://www.cgiar-csi.org/). The vegetation distribution information was obtained from a digitized 1:1,000,000 vegetation map of China (Chinese Academy of Sciences, 2001). We assumed there were no changes in the terrain and vegetation distribution on the plateau during the study period.

2.3. Vegetation EGS retrieval methodology

Many methods for retrieving vegetation phenophase information have been developed based on time series of remote sensing data, although these methods generally follow similar procedures, as described below. First, various functions, such as the asymmetric Gaussian functions (Jonsson and Eklundh, 2002), logistic functions (Shen et al., 2011; Zhang et al., 2003, 2006; Zhang and Goldberg, 2011), harmonic analysis of time series (HANTS) algorithms (Cong et al., 2012; White et al., 2009; Zhong et al., 2010) or six-time polynomials (Cong et al., 2012; Jeong et al., 2011; Piao et al., 2011), are used to fit or smooth the preprocessed NDVI or LAI data. Then, algorithms that set a threshold (Cong et al., 2012; Piao et al., 2006, 2011; White et al., 2009; Zhong et al., 2010) or use the rate of change in the curvature (Shen et al., 2011; Zhang et al., 2003, 2006; Zhang and Goldberg, 2011) are applied to detect the phenology based on the fitted or smoothed LAI data.

A similar approach was used in this study. However, the function used to fit LAI data is newer. This method integrates a logistic function and an asymmetric Gaussian function and uses the following function form:

$$y(t) = \frac{p}{1 + e^{m(t)}} + q, \quad (1)$$

where $m(t) = a \cdot t^2 + b \cdot t + c$; y is LAI-fitted value; t is time in day; q is the minimum of LAI value; $p + q$ is the maximum of LAI value; and a, b and c are parameters of the curve and control the position of inflexion points as well as the slope of the curve.

Here, we call Eq. (1) an *S*-curve function. Two special cases are worth considering. One is that when $m(t) = b \cdot t + c$ ($a = 0$, $b \neq 0$), Eq. (1) is equivalent to a logistic function (Zhang et al., 2003); the other case is that when $m(t) = a(t + (b/2a))^2$ ($b^2 = 4ac$, $a \neq 0$), Eq. (1) is equivalent to an asymmetric Gaussian function (Jonsson and Eklundh, 2002). Fig. 2a shows the comparison of fitted LAI which

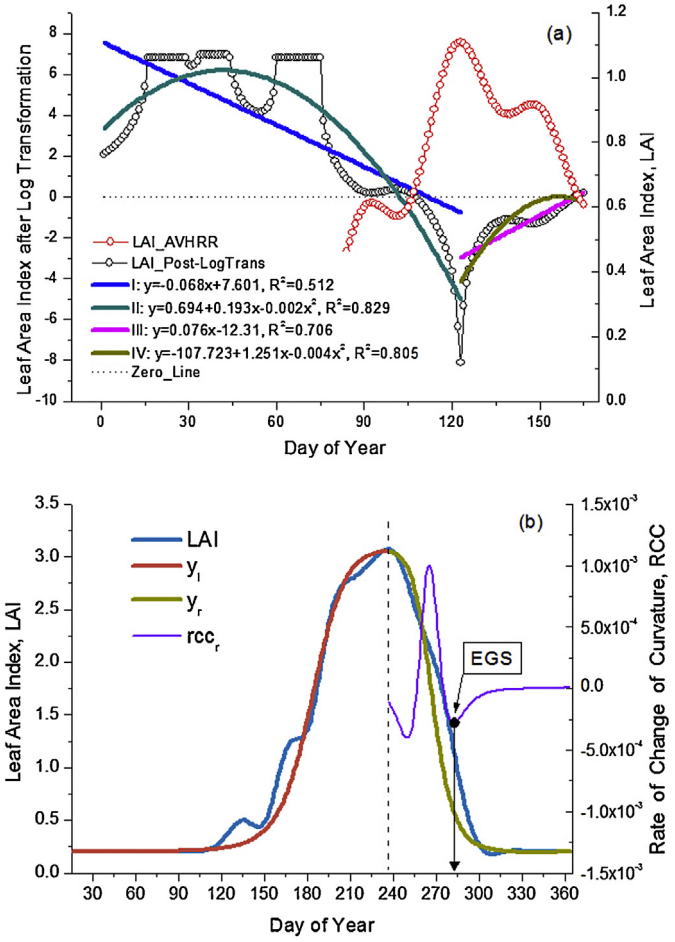

Fig. 2. Comparison of fitted LAI which after log transformation for *S*-curve function, logistic function and asymmetric Gaussian function (Lazi site, position: 29.10° N lat; 87.60° E lon; first half of 2004) (a), and calculation schematic of the end date of the growing season (EGS) (Haibei site, position: 37.08° N lat; 101.08° E lon; year: 2004) (b). The LAI data are processed using cubic spline interpolation in both subfigures. In subfigure (a), lines I and III are results of the logistic function. Line IV is the result of the asymmetric Gaussian function. Lines II and IV are results of the *S*-curve function. In subfigure (b), y_l(y_r) is the fitted value of the left (right) *S*-curve function; the rcc_r is the rate of change in the curvature of the right *S*-curve function.

after log transformation for *S*-curve function, logistic function and asymmetric Gaussian function. We can see the quadratic polynomial (lines II and IV) has a better performance for fitting LAI which after log transformation than the linear function (lines I and III). The difference between lines II and IV was repeated roots existing in the quadratic polynomial or not. Therefore, the *S*-curve function was more valid for fitting LAI than the logistic function and the asymmetric Gaussian function.

The seasonal variation of vegetation on the Qinghai–Tibetan Plateau in fewer area has two peaks in a given year (Fig. 2a). But in most area, the unique peak is dominant in a given year (Fig. 2b). Therefore, we use a piecewise *S*-curve function to fit the LAI value (Fig. 2b), in which the left part of the curve represents the spring phenology and the right portion indicates the autumn phenology. Its functional form is:

$$y(t; p, q, a, b, c) = \begin{cases} y_l(t; p_l, q_l, a_l, b_l, c_l) & t \le T \\ y_r(t; p_r, q_r, a_r, b_r, c_r) & t > T \end{cases}, \quad (2)$$

where y is LAI fitted value; t is time in days; y_l and y_r are the left-hand-side and right-hand-side LAI fitted values, respectively; T is time in days when LAI reaches its maximum; and $(p_l, q_l, a_l, b_l, c_l)$ $(p_r, q_r, a_r, b_r, c_r)$ are the set of parameters for the left-hand-side and the right-hand-side of the *S*-curve function, respectively. For obtaining the parameters a_r, b_r, c_r, the ordinary least square method can be used by inputting LAI data. The time frequency of AVHRR LAI is half monthly, and the data point number in a year was only 24. If the LAI time series is divided into two parts by a break point of LAI maximum, the number in either part will be even smaller. And the parameters obtained based on the less LAI data points are unreliable. The LAI fitted by *S*-curve function are of course less accurate or inaccurate. So before fitting the *S*-curve function, the AVHRR LAI data are needed to be interpolated to 1 day time scale first.

We then use the change rate of curvature (RCC) method of Zhang et al. (2003) to detect the vegetation phenology. First, the curvature of the *S*-curve function is calculated:

$$k = \frac{y''}{(1 + y'^2)^{3/2}}, \quad (3)$$

The variable y' or y'' is the first or second derivative of the *S*-curve function, respectively, as in Eqs. (4) and (5):

$$y' = -\frac{pz(2at + b)}{(1 + z)^2}, \quad (4)$$

$$y'' = -pz\frac{(2at + b)^2(1 - z) + 2a(1 + z)}{(1 + z)^3}, \quad (5)$$

where $z = e^{at^2 + bt + c}$.

The RCC is calculated based in Eq. (3). The two minima of the RCC are shown in Fig. 2b. The timing of the second minima of the RCC (rcc_r in Fig. 2b) can represent the EGS. In contrast to the direct use of the extreme value of the curvature, the EGS values obtained using this RCC method are later than the former and are much closer to the real end dates of the vegetation growing season. Finally, the EGS values of all pixels for the Qinghai–Tibetan Plateau can be calculated using the RCC method.

2.4. Validation

Validation of remote sensing retrievals is an important but difficult task. In particular, due to the lack of the in situ phenology observational data for autumn in the Qinghai–Tibetan Plateau, it is difficult to validate the accuracy of the retrieved results of EGS. However, the accuracy of the retrieved results can be alternatively determined by observed GPP data. GPP is the rate at which the vegetation captures and stores a given amount of chemical energy as biomass in a given length of time. However, GPP is largely dependent on the synthesis of organic material by the vegetation, i.e., green leaves of vegetation must be present. In autumn, when leaves begin falling, GPP decreases and reaches its minimum when the leaves have all fallen.

Moreover, the method of comparison with previous studies is also used to help justify the rationality of our retrieved results of EGS.

2.5. Correlation and trend analysis

To analyze the relationship between EGS and altitude throughout the entire plateau, the "*Reclassify*" tool in ArcGIS of version 9 was used to reclassify the DEM by equal interval method (100 m) to create the reclassification map first, which was noted as DEM_{rc}. Then, the mean of EGS during 1982–2011 was calculated and noted as $\bar{EGS}$. After that, the corresponding EGS was extracted by the meadow vegetation type and noted as $\bar{EGS}_{meadow}$. Finally, the "*Zonal Statistics*" tools in ArcGIS was used to get the relationship between EGS and altitude by inputting DEM_{rc} and $\bar{EGS}_{meadow}$. Next, a simple linear regression model was used to calculate the trend of EGS changes along altitude. And the Pearson correlation coefficient approach was used to calculate the correlation between them.

To study the relation between EGS spatial changes and climate factors, the mean of monthly air temperature, monthly total precipitation and monthly sunshine duration at each meteorological station during 1982–2011 was calculated respectively first, and separately noted as $\bar{T}_i$, $\bar{P}_i$, $\bar{H}_i$ (the subscript i is the meteorological station ID). Then, the mean of EGS during 1982–2011 was calculated, and noted as $\bar{EGS}$. After that, the corresponding EGS (noted as $\bar{EGS}_i$, the subscript i is the meteorological station ID) at each meteorological station was obtained from $\bar{EGS}$ using the coordinates (lat, lon) of the station. Finally, the simple linear regression method and the Pearson correlation coefficient were both used to analyze the relationships of the array $(\ldots, \bar{EGS}_{i-1}, \bar{EGS}_i, \bar{EGS}_{i+1}, \ldots)$ with the array $(\ldots, \bar{T}_{i-1}, \bar{T}_i, \bar{T}_{i+1}, \ldots)$, $(\ldots, \bar{P}_{i-1}, \bar{P}_i, \bar{P}_{i+1}, \ldots)$, and $(\ldots, \bar{H}_{i-1}, \bar{H}_i, \bar{H}_{i+1}, \ldots)$, respectively (the subscript i traversed all stations ID).

To detect the trend turning points of EGS during 1982–2011 at the regional scale, the Mann–Kendall (MK) method (Gocic and Trajkovic, 2013; Hamed and Rao, 1998; Mann, 1945) was used. Then the sub-periods were divided by those trend turning points. And the tends of EGS annual changes using the simple linear regression methods were analyzed during these subperiods.

To analyze the relation of annual EGS changes with climate factors, first using the coordinates (lat, lon) at individual meteorological stations, the corresponding EGS noted as $EGS_{i,j}$ (the subscript i is the meteorological station ID, the subscript j is year) of the station during 1982–2011 was obtained. Then, the mean of $EGS_{i,j}$ for all stations was calculated for each year, and noted as $\bar{EGS}_j$ (the subscript j is year). After that, the mean of monthly air temperature, monthly precipitation, monthly sunshine duration for all stations was calculated for each year, respectively, and separately noted as $\bar{T}_j$, $\bar{P}_j$ and $\bar{H}_j$ (the subscript j is year). Finally, the simple linear regression method and the Pearson correlation coefficient were both used to describe the relationships of the array $(\ldots, \bar{EGS}_{j-1}, \bar{EGS}_j, \bar{EGS}_{j+1}, \ldots)$ with the array $(\ldots, \bar{T}_{j-1}, \bar{T}_j, \bar{T}_{j+1}, \ldots)$, $(\ldots, \bar{P}_{j-1}, \bar{P}_j, \bar{P}_{j+1}, \ldots)$ and $(\ldots, \bar{H}_{j-1}, \bar{H}_j, \bar{H}_{j+1}, \ldots)$, respectively (the subscript j is year and varies in different study periods).

Moreover, a simple linear regression model was also used to analyze the comparison between AVHRR LAI and the LAI fitted using *S*-curve function.

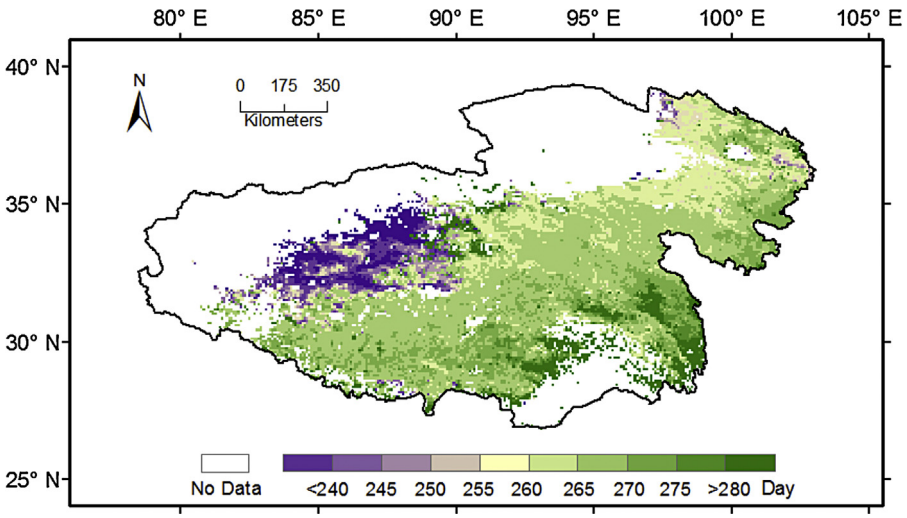

Fig. 3. Spatial distribution of the end dates of the growing season (EGS) averaged from 1982 to 2011 on the Qinghai–Tibetan Plateau.

In addition, a *t* test was used to test the significance of the simple linear regression coefficients and correlate coefficient, and *p* values <0.1, 0.05 and 0.01 are considered to be significant at the low, middle and high levels, respectively.

3. Results

3.1. Spatial patterns of the EGS

The spatial distribution of the EGS averaged over the last 30 years throughout the Qinghai–Tibetan Plateau is shown in Fig. 3. Overall, the EGS values range between early September and mid-October. The EGS date gradually decreased from southeast to northwest. The profiles of EGS spatial patterns are in agreement with the approximate vegetation distributions as shown in Fig. 1, especially for meadows. This is consistent with previous studies (such as Ding et al., 2012; Jin et al., 2013). Furthermore, the statistical analysis of EGS based on the vegetation type indicates that the EGS of meadow areas occurred in mid-September and mid-October and was later than in steppe areas, where the EGS starts in early September and mid-September. These results indicate that vegetation EGS was closely related to the vegetation type.

The spatial distribution of EGS also correlated with terrain. The meadow EGS changes with altitude negatively correlated with the DEM ($r^2 = 0.47$, $p < 0.001$, Fig. 4). The EGS was progressively earlier with increasing altitude, moving up by 3 days per 1000 m. This value is higher than the findings of Ding et al. (2012), who reported the EGS was advanced (the term 'advance' here and below means 'the date of EGS occurs earlier') by 1 day per 1000 m. The EGS changes at each altitude level are also evident, especially when the elevation is less than 4100 m (Fig. 4), suggesting that the distribution of the EGS may also be influenced by other factors, such as climate.

The linear correlation between the EGS and monthly climate factors is shown in Table 1. We observed a positive correlation between the EGS and monthly air temperature. In September, the correlation was highly significant ($p < 0.01$). In addition, this correlation in August had a mid-level significance ($p < 0.05$). However, in June and July, the correlation had a low significance ($p < 0.1$). Compared with air temperature, precipitation was a more important driver regarding the spatial distribution of the EGS. A significantly positive correlation ($p < 0.05$) between the EGS and monthly precipitation can be clearly seen in Table 1 with the exception of August ($p < 0.1$). Among all climate factors, sunshine duration was the dominant factor. The EGS was gradually advanced as the sunshine duration increased, with the EGS advancing by approximately 3 days per 10 h.

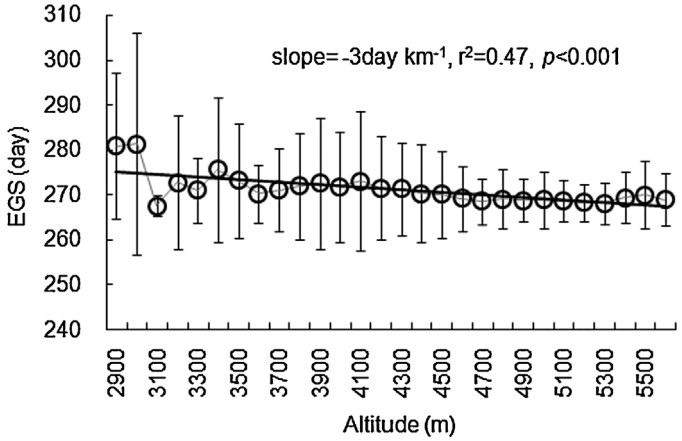

Fig. 4. The changes with altitude of area-averaged end dates of the growing season (EGS) of the meadow during 1982–2011. Error bars show standard deviation (SD) of EGS at each altitude level.

3.2. Inter-annual variations in the EGS

3.2.1. Changes at the regional scale

The inter-annual variations of EGS at the regional scale from 1982 to 2011 are illustrated in Fig. 5. During the entire study period, the positive EGS trend for all vegetation types was insignificant (slope = 0.041 day yr^{-1}, $r^2 = 0.103$, $p = 0.084$). The positive EGS trends for meadow and steppe vegetation were also insignificant (Fig. 5). To evaluate the long-term changes in the EGS, we

Table 1
Coefficients of correlation (*r*) between the spatial patterns of the end dates of the growing season (EGS) and monthly climate factors for the 46 valid meteorological stations shown in Fig. 1.

Climate factors	June	July	August	September
Air temperature (°C)	0.281*	0.252*	0.290*	0.395***
Precipitation (mm)	0.337**	0.369**	0.260*	0.480***
Sunshine duration (h)	−0.738***	−0.816***	−0.792***	−0.694***

* Indicates low significance level ($p < 0.1$).
** Indicates middle significance level ($p < 0.05$).
*** Indicates high significance level ($p < 0.01$)

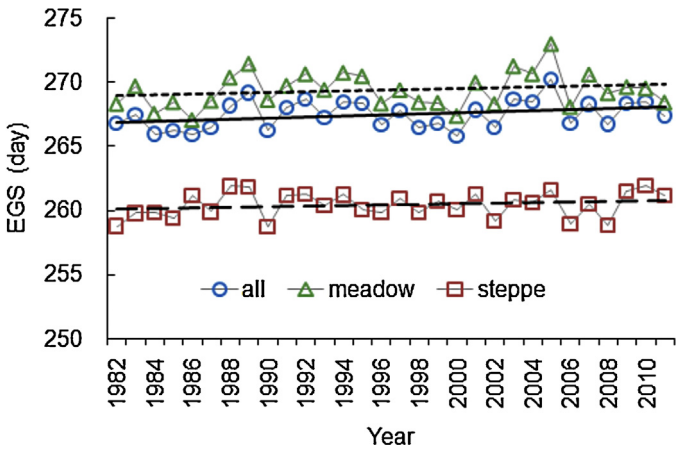

Fig. 5. Inter-annual variations of area-averaged end dates of the growing season (EGS) of the meadow, steppe and all vegetation on the Qinghai–Tibetan Plateau during 1982–2011. The black solid line shows the trend for all vegetation types (slope = 0.041 day yr^{-1}, r^2 = 0.103, p = 0.084). The black dotted line shows the trend for meadow vegetation (slope = 0.033 day yr^{-1}, r^2 = 0.045, p = 0.259). The black dashed line shows the trend for steppe vegetation (slope = 0.022 day yr^{-1}, r^2 = 0.037, p = 0.305).

calculated the EGS trend turning points for all vegetation types using the MK trend test method. As shown in Fig. 6, three distinctly different trends during 1982–1994, 1994–1999 and 1999–2011 were identified. The EGS was clearly delayed (slope = 0.155 day yr^{-1}, r^2 = 0.293, p = 0.045) prior to the year 1994. Subsequently, the EGS was advanced (slope = −0.373 day yr^{-1}, r^2 = 0.595, p = 0.049) until the year 1999. During the last period (1999–2011), the EGS was again gradually delayed (slope = 0.096 day yr^{-1}, r^2 = 0.097, p = 0.3). Similar trends were also observed for the meadow and steppe before and after the turning points (1994 and 1999).

3.2.2. Spatial patterns of trends in EGS

The spatial patterns of trends in the vegetation EGS are described in Fig. 7. There was a strong spatial heterogeneity throughout the plateau for the four different periods. During the entire study period (Fig. 7a), the trend was not obvious but increased slightly. The pixels below −0.1 day yr^{-1} account for 13.8% of the total; those varying from −0.1 day yr^{-1} to 0.1 day yr^{-1} account for 62.0% of the total, and those pixels above 0.1 day yr^{-1} account for 24.2% of the total. The pixel for which the declining trend was significant (<−0.1 day yr^{-1}, p < 0.05) corresponds to approximately 4.1% of the total, and these pixels were dispersed throughout the study area. The area with a significant increasing trend (>0.1 day yr^{-1}, p < 0.05) accounts for approximately 9.3% of the total and is distributed mainly in the eastern region of the plateau, including most of the Changdu, Yushu and Naqu Prefectures.

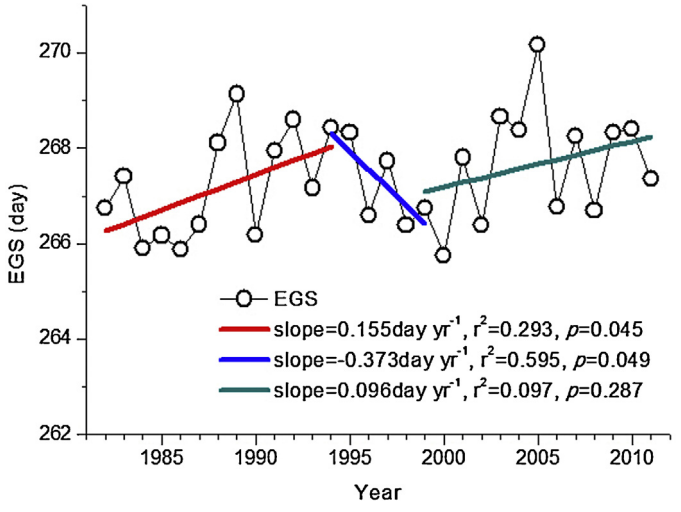

Fig. 6. Trends of annual changes of end dates of the growing season (EGS) for all vegetation types during 1982–2011 on the Qinghai–Tibetan Plateau. The trend turning points determined by the Mann–Kendall test are the years of 1994 and 1999.

During the period of 1982–1994, the significant increasing trend through the plateau can be observed (Fig. 7b). The pixels greater than 0.1 day yr^{-1} account for 54.4% of the total, and the pixels less than −0.1 day yr^{-1} only account for 22.0% of the total. Moreover, pixels having a significant increasing trend (>0.1 day yr^{-1}, p < 0.05) account for approximately 11.0% of the total and were mainly distributed east of the plateau and southeast of Yushu, Naqu and Ali Prefectures and north of Shannan Prefecture; these pixels are 4-fold more numerous than those showing a significant decline (<−0.1 day yr^{-1}, p < 0.05).

For the period of 1994–1999, there was a clear decreasing trend throughout the entire plateau. As shown in Fig. 7c, 54.3% of pixels have values less than −0.1 day yr^{-1}, and these pixels are approximately 1.5-fold more numerous than those greater than 0.1 day yr^{-1}. In addition, the proportion of significantly decreasing pixels (<−0.1 day yr^{-1}, p < 0.05) is 8.0%; these were mainly distributed in Guoluo, Yushu, Changdu and southeast of Naqu Prefecture and are 2-fold more abundant than the significantly increasing pixels (>0.1 day yr^{-1}, p < 0.05).

For the final period corresponding to 1999–2011, increasing and decreasing trends were observed (Fig. 7d). Approximately 39.9% of pixels on the plateau have an increasing trend, and approximately 31.2% of pixels show a decline. Based on the trend significance (p < 0.05) test, approximately 5.6% of pixels show an increasing trend, which is slightly higher than the proportion of pixels having a decreasing trend.

3.2.3. Correlation with climate factors

To understand the inter-annual variations of the EGS for different study periods, as mentioned above, the relationship between the annual change of the EGS and climate factors was analyzed. The correlations between the EGS and climate factors are diverse among the various months for different study periods (Table 2).

During the study period (1982–2011), the correlation between the EGS and air temperature is positive in June and September but negative in July and August. However, none of these correlations are significant. At the same time, the correlation between the EGS and precipitation is negative in June and September but positive in July and August; however, the correlation in June and August has a low level of significance (p < 0.1). The correlation between the sunshine duration and EGS is positive in June and September but negative in July and August. Similar to the precipitation, the correlation in June and August has a low significance (p < 0.1).

During other study periods, the influences of climate factors on the EGS are very complex (Table 2), although the negative effects of air temperature and sunshine duration on vegetation growth in summer and positive effects in autumn can be identified. In addition, the positive effects of precipitation on vegetation growth in summer and negative effects in autumn can also be identified.

4. Discussion

4.1. Validation of the EGS

As shown in Fig. 8a, there is a high level of consistency between the retrieved EGS result and the minima of the observed GPP in autumn. In addition, the AVHRR LAI and the fitted value of the

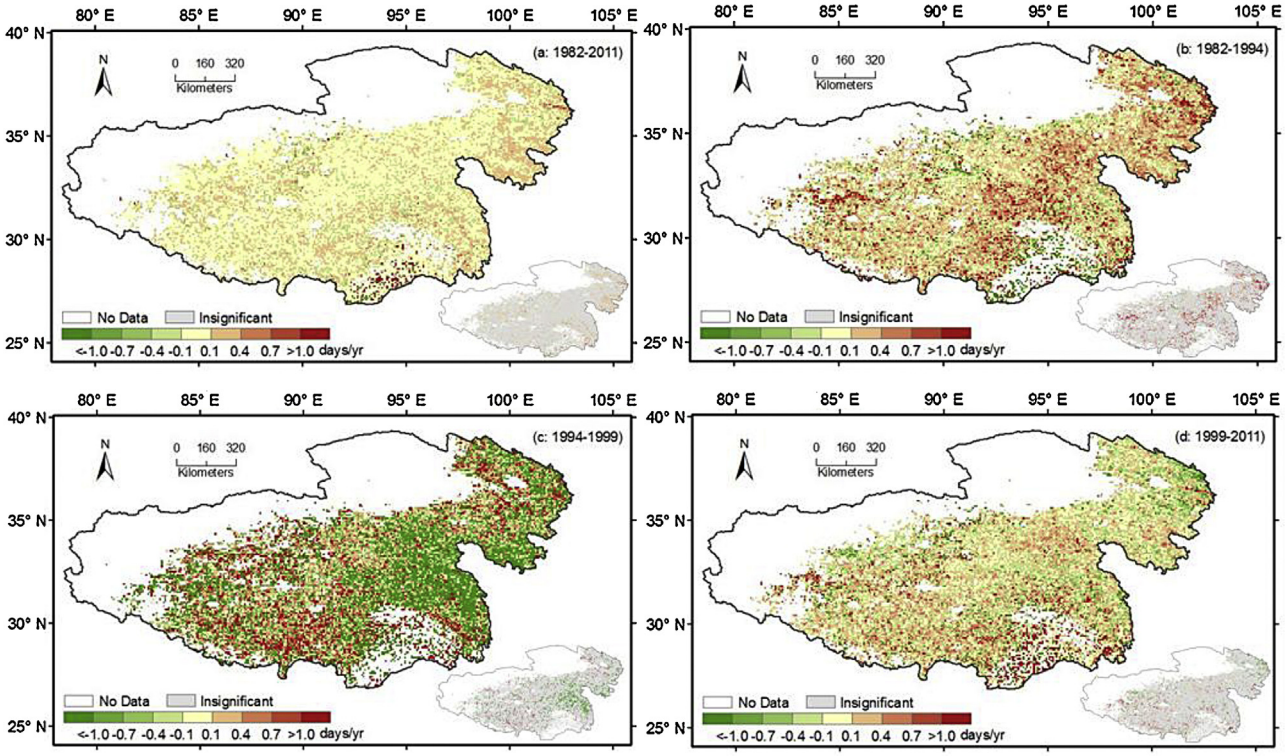

Fig. 7. Spatial patterns of trends at the end of the growing season (EGS) for four periods.

S-curve function are compared in Fig. 8b. The scatter plot between these data (slope = 0.972, $r^2 = 0.95$, $p < 0.001$) shows that the *S*-curve function has a great advantage in fitting the LAI data, and LAI variation in autumn also demonstrates the high accuracy of the EGS retrieved results.

In addition, the accuracy of the EGS retrieved results in this study was also assessed by comparison with previous studies. For example, the timing of the EGS (Fig. 3) throughout the plateau averaged over the past 30 years is similar to the previous findings of other studies (e.g. Ding et al., 2012; Jin et al., 2013; Yu et al., 2010). At the regional scale, the trend in the annual changes of the EGS during the period of 1982–1994 (Fig. 6) is in agreement with the results of Piao et al. (2006), who illustrated the vegetation autumn phenology of alpine meadows and tundra distributed mainly on the Qinghai–Tibetan Plateau from 1982 to 1994. In the following period of 1994–1999 (Fig. 6), the trend is also in agreement with the results of Piao et al. (2006). In the last period of 1999–2011 (Fig. 6), the trend is in accordance with the findings of Ding et al. (2012), and only the rate of increase (slope = 0.096 day yr^{-1}) is lower.

Admittedly, this qualitative examination of retrieved EGS values is less accurate than the quantitative analyses. However, it is the best and only available method when observational data are lacking. Such a situation occurs not only in this work but also in many other studies (Jeong et al., 2011; Piao et al., 2006, 2011; Shen et al., 2011). Moreover, even if we have in situ observational data, the validation of retrieved results remains quite difficult due to enormous spatial-scale differences between datasets (Shen et al., 2011; Zhang and Goldberg, 2011). Therefore, as indicated by many studies, to adequately validate satellite-derived phenological metrics, studies (i.e., collecting the phenological observation data, and up-scaling

Table 2
Coefficients of correlation (r) between the annual changes in the end dates of the growing season (EGS) and the monthly climate factors for the 46 valid meteorological stations shown in Fig. 1 from 1982 to 2011.

Climate Factors	Periods	June	July	August	September
Air temperature (°C)	1982–2011	0.130	−0.181	−0.060	0.160
	1982–1994	0.789***	0.287	−0.387	0.093
	1994–1999	0.664	−0.661	−0.850**	0.461
	1999–2011	−0.305	−0.313	0.230	0.353
Precipitation (mm)	1982–2011	−0.339*	0.169	0.321*	−0.169
	1982–1994	−0.530*	−0.022	0.470	−0.291
	1994–1999	−0.235	0.105	0.237	0.301
	1999–2011	−0.248	0.308	0.437	−0.206
Sunshine duration (h)	1982–2011	0.313*	−0.064	−0.313*	0.238
	1982–1994	0.421	−0.177	−0.352	0.087
	1994–1999	0.168	0.117	−0.335	−0.036
	1999–2011	0.366	−0.119	−0.572*	0.367

* Indicates low significance level ($p < 0.1$).
** Indicates middle significance level ($p < 0.05$).
*** Indicates high significance level ($p < 0.01$)

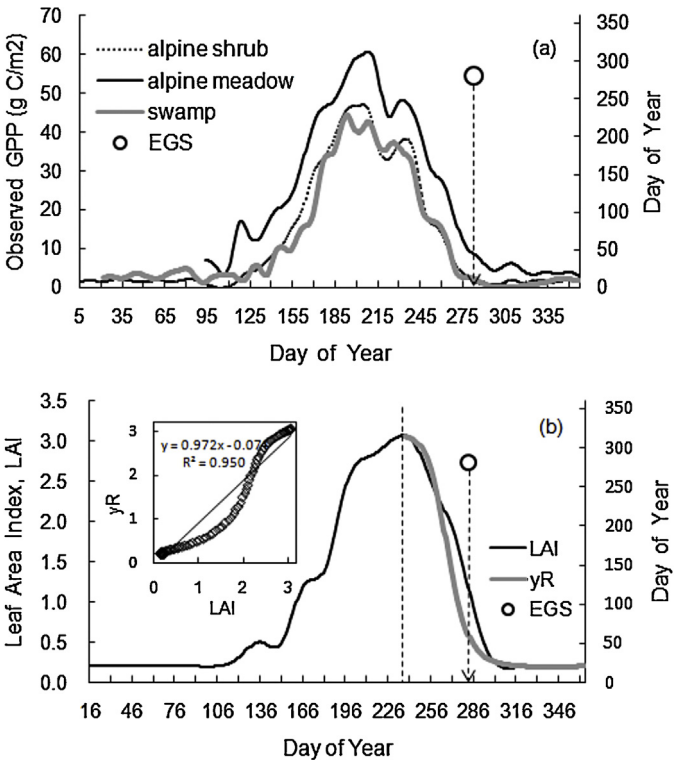

Fig. 8. Validation for the end date of the growing season (EGS) by applying the observed gross primary production (GPP) data at the Haibei eddy flux tower site (position: 37.08° N lat; 101.08° E lon; year: 2004) (a), and the comparison between the AVHRR LAI and the fitted value of the *S*-curve function at the same site (b). The three types of GPP and LAI data are all processed using cubic spline interpolation. The *yR* is the fitted value of the right *S*-curve function.

the observed data from the individual plant to landscape level) based on ground observations must be performed in the future.

4.2. Influences of climate factors on the EGS

This paper presents the spatial and temporal variations of EGS on the Qinghai–Tibetan Plateau.

First, regarding the spatial variation of EGS, it is well known that air temperature affects the phenological development of plants (Snyder et al., 2001), and a positive correlation between EGS and monthly air temperature was observed (Table 1). Furthermore, this correlation in September is highly significant (slope = 2.148, $p = 0.007$). In the Qinghai–Tibetan Plateau, the highest monthly air temperatures occur from June to August. The vegetation grows rapidly during this period, and the LAI reaches its peak in August. Therefore, the air temperature in this phase has a weak effect on the EGS. From September, the air temperature begins to decline. Because leaf senescence related to temperate is mainly modulated by cumulative cold temperatures below a certain threshold temperature (Jeong et al., 2011; Richardson et al., 2006), a warmer air temperature in autumn can lead to a delay in the EGS. Thus, based on the spatial distribution of the air temperature in September (declining from southeast to northwest), the vegetation density displays corresponding changes (Zhong et al., 2010), and the EGS displays similar spatial patterns.

Compared with air temperature, the impact of precipitation on the EGS is much stronger (Table 1). As noted by Zhou et al. (2007), spatial variation in vegetation is mainly affected by precipitation in this area. On the Qinghai–Tibetan Plateau, the maximum precipitation occurs mainly in July and August. From June to August, the vegetation grows vigorously due to warm temperatures and an adequate supply of water. After August, with decreasing precipitation, the importance of precipitation for vegetation growth becomes increasingly important. Therefore, because of the spatial distribution of the precipitation (decreasing from southeast to northwest (Ye et al., 2013)), the EGS also presents similar spatial patterns.

At the same time, the sunshine duration also plays an important role in the spatial distribution of the EGS (Table 1). The significantly negative correlation between the EGS and monthly sunshine duration is in agreement with the findings of Mao et al. (2007), who reported a significant negative correlation between the NDVI and sunshine duration. Due to the high elevation and small extent of cloud cover on the Qinghai–Tibetan Plateau, illumination is very abundant. However, excessive sunshine may increase surface evapotranspiration, which aggravates the drought conditions of the plateau. Moreover, the excessive solar radiation produced by excessive sunshine also inhibits vegetation growth. Thus, the EGS displays an inverse relationship with the spatial distribution of the sunshine duration (increasing from southeast to northwest) (Hua et al., 2009).

The correlations between climate factors and the temporal variation of the EGS are very complex (Table 2). These correlations indicate that in July and August, the air temperature may restrain the vegetation growth, whereas in June and September, the opposite effect occurs. As is observed for the sunshine duration. But precipitation has an opposite effect compared to air temperature. The regression analyses indicate that the influence of the monthly air temperature on the annual changes in the EGS is limited during the overall study period, as is observed during the period of 1999–2011. However, from 1982 to 1994, there is a significant positive correlation between annual changes in the EGS and the air temperature in June. In June, the air temperature averaged over this 13-year period is approximately 11.1 °C and increases at a rate of 0.042 °C yr^{-1}. With increasing air temperature, the suitable temperature can enhance the development of plants after revival during this phase. Therefore, the EGS of plants, which are healthy and strong in this phase, may occur later in the following autumn. During the period of 1994–1999, the annual changes in the EGS were mainly influenced by the air temperature during August. The averaged air temperature was approximately 12.3 °C and increased at a rate of 0.025 °C yr^{-1} during this period. With increasing air temperature, the higher temperature may result in a decreased water content in the soil and plants, which thus restricts the vegetation growth and leads to an advanced EGS in autumn.

In contrast to air temperature, precipitation is essential for plant growth. During the entire study period, there was a low significant correlation between precipitation and annual changes in the EGS in June and August (Table 2). In June, the precipitation averaged over 30 years was approximately 67.8 mm. A strong trend was not evident during this period. The precipitation usually reached its annual peak In August. The mean precipitation for the 30-year period is approximately 79.7 mm with a low significance ($p = 0.076$, slope = 0.567 mm yr^{-1}). Therefore, the increasing precipitation may promote effective vegetation growth and then delay the senescence of vegetation in the following September. During the period of 1982–1994, the low-significance correlation only occurs in June, which has the highest correlation level of all months. In this period, the precipitation level slowly decreased. However, the precipitation continued to facilitate plant growth when the air temperature was suitable. For the periods of 1994–1999 and 1999–2011, no significant correlation was found. However, the air temperature, as discussed above, and the sunshine duration played important roles in the annual variations in the EGS during these two periods.

During 1982–2011, the correlation between the annual changes in the EGS and the sunshine duration showed a low significance level in June and August. The sunshine duration trend is not

obvious in June (slope = −0.227 h yr^{-1}, $p = 0.11$) but is significant in August (slope = −0.187 h yr^{-1}, $p = 0.008$). Thus, the decreased sunshine duration in August not only weakens the solar radiation but also regulates the level of soil surface evaporation to maintain vegetation survival. During the following two sub-periods (1982–1994 and 1994–1999), the influence of the sunshine duration on annual variations in the EGS was limited with no significant correlations, whereas during the last period of 1999–2011, there was a low-significance correlation with the sunshine duration in August. However, the trend of sunshine duration during this period was not evident.

Many studies have been conducted on the relationship of phenology with climate factors, although few studies have reported on the influences of climate factors on autumn phenology. Autumn phenology is a more complex process than spring phenology (Chmielewski and Rötzer, 2001), and achieving a sufficient understanding of the long-term autumn phenology variations is very difficult (Jeong et al., 2011). Our results only present an approximate correlation between climate factors and the EGS to explain the EGS variations. These detailed relationships require further analysis. In addition, the EGS variations may be affected by other factors, such as extreme weather events, grassland degradation, thawing–freezing processes, human activities and their combined effects. Therefore, these factors must also be considered in future work.

4.3. Uncertainties of the results

Although our results on the spatial and temporal variations of EGS are similar to those of previous studies, the differences among them should not be ignored. These differences may be attributed to variations in the study areas, study periods, datasets and methods for deriving the phenology.

Inconsistencies due to the use of different study areas were discussed in the introduction of this paper. Study period differences usually affect the trends of inter-annual changes in the EGS. It is clear that the trends in the phenology time series data vary with the length of data series. This variation is most evident when a phenology turning point is observed. Therefore, the trends derived from long-term EGS data should be more reliable than those from short-term data. The time scale of our results spanned 30 years, which is longer than any previous studies (Ding et al., 2012; Jin et al., 2013; Piao et al., 2006; Yu et al., 2010). Therefore, the uncertainties of our results should be smaller. The uncertainties of the EGS are also correlated with datasets. Based on previous studies, uncertainty has been shown to generally involve AVHRR NDVI data, MODIS (moderate resolution imaging spectroradiometer) NDVI data and SPOT-VGT NDVI data. Many studies have reported that spring phenology trends derived from AVHRR and MODIS data differ enormously over the past decade (Ding et al., 2012; Zeng et al., 2011; Zhang et al., 2013). In addition, differences in the autumn phenology derived from AVHRR and MODIS data are clear (Zeng et al., 2011). Based on the temporal frequency and spatial resolution, MODIS (8-day interval, 1 km resolution) data and SPOT-VGT (10-day interval, 1 km resolution) data are superior to AVHRR data. However, for long-term series, AVHRR data are unique and undoubtedly the most reliable. Many methods are used to retrieve vegetation phenology from satellite data, although none of them have been universally validated. In addition, a comprehensive inter-comparison and interpretation of those methods has not been conducted (White et al., 2009). Thus, the selection of a robust method to retrieve phenology is urgently needed (White et al., 2009). In this paper, we used the *S*-curve function, which integrates a logistic function and an asymmetric Gaussian function, to fit the LAI data and use the rate of change in the curvature (RCC) to determine the end dates of the growing season. Compared with the logistic function and asymmetric Gaussian function, the *S*-curve function showed a better performance for fitting the LAI data. Therefore, the EGS recognition capability of the EGS based on the *S*-curve function is higher than of the other functions. In addition, because the RCC method does not require the parameters beforehand, in contrast to the threshold method, it can reduce the bias due to human subjective factors. However, due to the absence of in situ phenological observation data, it is difficult to thoroughly evaluate the retrieval results of the *S*-curve function.

Furthermore, the climate data used in this paper were obtained from in situ data. Although these data can provide accurate meteorological information, when we estimate regional features using such data, uncertainty is inevitable due to the complexity of the underlying surface of the entire plateau.

5. Conclusion

In this study, we used the rate of the change in the curvature of the *S*-curve function to extract the end dates of the growing season from a long-term series of AVHRR LAI data. We then determined the spatial and temporal variations of the EGS. The following conclusions are drawn:

(1) The vegetation EGS, averaged from 1982 to 2011,occurred between early September and the middle of October on the Qinghai–Tibetan Plateau. The EGS gradually decreased from southeast to northwest.
(2) The spatial patterns of the EGS were closely related to the vegetation type, the terrain and climate factors. With increasing altitude, the EGS advanced at a rate of approximately 3 days per 1000 m. In addition, the spatial distribution of the EGS varied in accordance with the patterns of air temperature and precipitation but showed an inverse trend with respect to the sunshine duration.
(3) The trend of EGS delaying at the regional scale was less pronounced throughout the study period. By analyzing the trend turning point, we found that the EGS was significantly delayed during the first period (1982–1994) at a rate of 2 days per decade, and during the following period (1994–1999), it advanced at a rate of 4 days per decade. However, from 1999 to 2011, the EGS was non-significantly delayed again at a rate of 1 day per decade.
(4) The spatial patterns of the trends of EGS annual changes were diverse during the different periods. From 1982 to 2011, the EGS trend increased slightly but not significantly. During 1982–1994, the area having pixels with an increasing trend is large, and pixels with a significant increasing trend are mainly distributed east of the plateau, southeast of the Yushu, Naqu and Ali Prefectures and north of the Shannan Prefecture. During the period of 1994–1999, a decreasing trend was readily observed. In addition, pixels having a significant decreasing trend are mainly located in Guoluo, Yushu, Changdu and southeast of the Naqu Prefecture. For the last period of 1999–2011, increasing and decreasing trends are both apparent, although their distributions are scattered.
(5) An analysis of the correlation between annual changes in the EGS and climate factors revealed that the former negatively correlated with precipitation ($p < 0.1$) in June, but positively with precipitation ($p < 0.1$) in August during 1982–2011. As the same time, the former also positively correlated with sunshine duration ($p < 0.1$) in June, yet negatively with sunshine duration ($p < 0.1$) in August. The correlation between annual changes of EGS and monthly air temperature was not found during this phase. During 1982–1994, the annual changes of EGS positively

correlated with air temperature ($p < 0.01$) and negatively with precipitation ($p < 0.1$) in June. During 1994–1999, the annual changes of EGS only negatively correlated with air temperature ($p < 0.05$) in August. During 1999–2011, the annual changes of EGS only negatively correlated with sunshine duration ($p < 0.1$) in August.

Acknowledgements

This research is supported by a research grant of Key Project for the Strategic Science Plan in IGSNRR, CAS (Grant no. 2012ZD010), a Research Plan of LREIS (O88RA900KA), CAS, the research grants (41071059 and 41271116) funded by the National Science Foundation of China, a research grant named "Adaptation of Asia-Pacific Forests to Climate Change" (Project #APFNet/2010/PPF/001) founded by the Asia-Pacific Network for Sustainable Forest Management and Rehabilitation, the Strategic Priority Research Program "Climate Change: Carbon Budget and Related Issues" of the Chinese Academy of Sciences (Grant no. XDA05040403) and "One Hundred Talents" program funded by the Chinese Academy of Sciences. We thank Dr. Ranga B. Myneni, Dr. C.J. Tucker and Dr. J. Pinzon of NASA GSFC for making available the GIMMS NDVI3g data set. And, we also thank Dr. Nicholas C. Coops for his valuable comments and suggestions which have helped us to improve the manuscript.

References

Borak, J., Jasinski, M., 2009. Effective interpolation of incomplete satellite-derived leaf-area index time series for the continental United States. Agricultural and Forest Meteorology 149, 320–332.

Chmielewski, F.M., Rötzer, T., 2001. Response of tree phenology to climate change across Europe. Agricultural and Forest Meteorology 108, 101–112.

Cleland, E.E., Chuine, I., Menzel, A., Mooney, H.A., Schwartz, M.D., 2007. Shifting plant phenology in response to global change. Trends in Ecology and Evolution 22 (7), 357–365.

Cong, N., Wang, T., Nan, H.J., Ma, Y.C., Wang, X.H., Myneni, R.B., Piao, S.L., 2012. Changes in satellite-derived spring vegetation green-up date and its linkage to climate in China from 1982 to 2010: a multimethod analysis. Global Change Biology 19 (3), 881–891.

Ding, M.J., Zhang, Y.L., Sun, X.M., Liu, L.S., Wang, Z.F., Bai, W.Q., 2012. Spatiotemporal variation in alpine grassland phenology in the Qinghai–Tibetan Plateau from 1999 to 2009. Chinese Science Bulletin 58 (3), 396–405.

Dong, M.Y., Jiang, Y., Zheng, C.T., Zhang, D.Y., 2012. Trends in the thermal growing season throughout the Tibetan Plateau during 1960–2009. Agricultural and Forest Meteorology 166–167, 201–206.

Gocic, M., Trajkovic, S., 2013. Analysis of changes in meteorological variables using Mann–Kendall and Sen's slope estimator statistical tests in Serbia. Global and Planetary Change 100, 172–182.

Hamed, K.H., Rao, A.R., 1998. A modified Mann–Kendall trend test for autocorrelated data. Journal of Hydrology 204, 182–196.

Hua, W., Fan, G.Z., Zhou, D.W., Chen, Q.L., 2009. Analysis on the variation trend of interannual and interdecadal seasonal sunshine duration over Tibetan plateau. Journal of Natural Resources 24 (10), 1810–1817 (in Chinese with abstract in English).

Jeong, S.J., Ho, C.H., Gim, H.J., Brown, M.E., 2011. Phenology shifts at start vs. end of growing season in temperate vegetation over the Northern Hemisphere for the period 1982-2008. Global Change Biology 17 (7), 2385–2399.

Jin, Z.N., Zhuang, Q.L., He, J.S., Luo, T.X., Shi, Y., 2013. Phenology shift from 1989 to 2008 on the Tibetan Plateau: an analysis with a process-based soil physical model and remote sensing data. Climatic Change, http://dx.doi.org/10.1007/s10584-013-0722-7.

Jong, R., Bruin, S., Wit, A., Schaepman, M.E., Dent, D.L., 2011. Analysis of monotonic greening and browning trends from global NDVI time-series. Remote Sensing of Environment 115, 692–702.

Jonsson, P., Eklundh, L., 2002. Seasonality extraction by function fitting to time-series of satellite sensor data. IEEE Transactions on Geoscience and Remote Sensing 40 (8), 1824–1832.

Kang, X.F., Fu, Y., Yan, L.D., Li, X.L., 2010. The relationship between plant communities of meadow grassland and climatic factors around north Qinghai Lake. Pratacultural Science 27 (10), 1–9 (in Chinese with abstract in English).

Li, Z.Q., Yu, G.R., Xiao, X.M., Li, Y.N., Zhao, X.Q., Ren, C.Y., Zhang, L.M., Fu, Y.L., 2007. Modeling gross primary production of alpine ecosystems in the Tibetan Plateau using MODIS images and climate data. Remote Sensing of Environment 107 (3), 510–519.

Liu, X.D., Chen, B.D., 2000. Climatic warming in the Tibetan Plateau during recent decades. International Journal of Climatology 20, 1729–1742.

Ma, L.Y., Huang, X.D., Fang, J., Liang, T.G., 2011. Temporal and spatial change of grassland vegetation index in Tibetan Plateau. Pratacultural Science 28 (6), 1106–1116 (in Chinese with abstract in English).

Mann, H.B., 1945. Nonparametric tests against trend. Econometrica 13, 245–259.

Mao, F., Lu, Z.G., Zhang, J.H., Hou, Y.Y., 2007. Relations between AVHRR NDVI and climate factors in Northern Tibet in recent 20 years. Acta Ecologica Sinica 27 (8), 3198–3205 (in Chinese with abstract in English).

Menzel, A., Estrella, N., Fabian, P., 2001. Spatial and temporal variability of the phenological seasons in Germany from 1951 to 1996. Global Change Biology 7, 657–666.

Menzel, A., Fabian, P., 1999. Growing season extended in Europe. Nature 397, 659.

Piao, S.L., Cui, M.D., Chen, A.P., Wang, X.H., Ciais, P., Liu, J., Tang, Y.H., 2011. Altitude and temperature dependence of change in the spring vegetation green-up date from 1982 to 2006 in the Qinghai–Xizang Plateau. Agricultural and Forest Meteorology 151 (12), 1599–1608.

Piao, S.L., Fang, J.Y., Zhou, L.M., Ciais, P., Zhu, B., 2006. Variations in satellite-derived phenology in China's temperate vegetation. Global Change Biology 12 (4), 672–685.

Pudas, E., Leppala, M., Tolvanen, A., Poikolainen, J., Venalainen, A., Kubin, E., 2008. Trends in phenology of *Betula pubescens* across the boreal zone in Finland. International Journal of Biometeorology 52 (4), 251–259.

Ran, Y.H., Li, X., Lu, L., 2009. China land cover classification at 1 km spatial resolution based on a multi-source data fusion approach. Advances in Earth Science 24 (2), 192–203 (in Chinese with abstract in English).

Rathcke, B.L., Elizabeth, P., 1985. Phenological patterns of terrestrial plants. Annual Review of Ecology and Systematics 16, 179–214.

Reich, P.B., 1995. Phenology of tropical forests: patterns, causes, and consequences. Canadian Journal of Botany 73 (2), 164–174.

Richardson, A.D., Bailey, A.S., Denny, E.G., Martin, C.W., O'Keefe, J., 2006. Phenology of a northern hardwood forest canopy. Global Change Biology 12 (7), 1174–1188.

Schwartz, M.D., 2003. Phenology: An Integrative Environmental Science. Kluwer Academic Publishers, Netherlands.

Shen, M.G., Tang, Y.H., Chen, J., Zhu, X.L., Zheng, Y.H., 2011. Influences of temperature and precipitation before the growing season on spring phenology in grasslands of the central and eastern Qinghai–Tibetan Plateau. Agricultural and Forest Meteorology 151 (12), 1711–1722.

Snyder, R.L., Spano, D., Duce, P., Cesaraccio, C., 2001. Temperature data for phenological models. International Journal of Biometeorology 45, 178–183.

White, M.A., Debeurs, K.M., Didan, K., Inouye, D.W., Richardson, A.D., Jensen, O.P., O'Keefe, J., Zhang, G., Nemani, R.R., Vanleeuwen, W.J.D., Brown, J.F., Dewit, A., Schaepman, M., Lin, X., Dettinger, M., Bailey, A.S., Kimball, J., Schwartz, M.D., Baldocchi, D.D., Lee, J.T., Lauenroth, W.K., 2009. Intercomparison, interpretation, and assessment of spring phenology in North America estimated from remote sensing for 1982–2006. Global Change Biology 15 (10), 2335–2359.

White, M.A., Thornton, P.E., Running, S.W., 1997. A continental phenology model for monitoring vegetation responses to interannual climatic variability. Global Biogeochemical Cycles 11 (2), 217–234.

Xu, Y.Y., Zhang, G.H., Yang, L.M., 2012. Detecting major phenological stages of rice using MODIS-EVI data and Symlet11 wavelet in Northeast China. Acta Ecologica Sinica 32 (7), 2091–2098 (in Chinese with abstract in English).

Ye, H., Wang, J.B., Huang, M., Qi, S.H., 2013. Spatial pattern of vegetation precipitation use efficiency and its response to precipitation and temperature on the Qinghai–Xizang Plateau of China. Chinese Journal of Plant Ecology 36 (12), 1237–1247 (in Chinese with abstract in English).

Yu, H.Y., Luedeling, E., Xu, J.C., 2010. Winter and spring warming result in delayed spring phenology on the Tibetan Plateau. Proceedings of the National Academy of Sciences of the United States of America 107 (51), 22151–22156.

Zeng, H.Q., Jia, G.S., Epstein, H., 2011. Recent changes in phenology over the northern high latitudes detected from multi-satellite data. Environmental Research Letters 6 (4), 1–11.

Zhang, G.L., Zhang, Y.J., Dong, J.W., Xiao, X.M., 2013. Green-up dates in the Tibetan Plateau have continuously advanced from 1982 to 2011. Proceedings of the National Academy of Sciences of the United States of America 110 (11), 4309–4314.

Zhang, X.Y., Friedl, M.A., Schaaf, C.B., 2006. Global vegetation phenology from Moderate Resolution Imaging Spectroradiometer (MODIS): evaluation of global patterns and comparison with in situ measurements. Journal of Geophysical Research 111, 1–14.

Zhang, X.Y., Friedl, M.A., Schaaf, C.B., Strahler, A.H., Hodges, J.C.F., Gao, F., Reed, B.C., Huete, A., 2003. Monitoring vegetation phenology using MODIS. Remote Sensing of Environment 84, 471–475.

Zhang, X.Y., Goldberg, M.D., 2011. Monitoring fall foliage coloration dynamics using time-series satellite data. Remote Sensing of Environment 115 (2), 382–391.

Zhong, L., Ma, Y.M., Salama, M.S., Su, Z.B., 2010. Assessment of vegetation dynamics and their response to variations in precipitation and temperature in the Tibetan Plateau. Climatic Change 103 (3–4), 519–535.

Zhou, R., Yang, Y.H., Fang, J.Y., 2007. Responses of vegetation activity to precipitation variation on the Tibetan plateau. Acta Scientiarum Naturalium Universitatis Pekinensis 43 (6), 771–775 (in Chinese with abstract in English).

Zhu, Z.C., Bi, J., Pan, Y.Z., Ganguly, S., Anav, A., Xu, L., Samanta, A., Piao, S.L., Nemani, R.R., Myneni, R.B., 2013. Global Data Sets of Vegetation Leaf Area Index (LAI) 3g and Fraction of Photosynthetically Active Radiation (FPAR) 3g Derived from Global Inventory Modeling and Mapping Studies (GIMMS) Normalized Difference Vegetation Index (NDVI3g) for the Period 1981 to 2011. Remote Sensing 5 (2), 927–948.